LC–TH–2002–002
hep-ph/0202109
February 2002

Complete electroweak one-loop radiative corrections to top-pair production at TESLA – a comparison* –

J. Fleischer[1†], T. Hahn[2], W. Hollik[3,4], T. Riemann[5],
C. Schappacher[3] and A. Werthenbach[5]

[1] Universität Bielefeld, Universitätsstrasse 25, D–33615 Bielefeld, Germany
[2] Fraunhofer-Institut für Integrierte Schaltungen, Am Weichselgarten 3, D–91058 Erlangen, Germany
[3] Universität Karlsruhe, Inst. für Theoretische Physik, Kaiserstrasse 12, D–76128 Karlsruhe, Germany
[4] Max-Planck-Institut für Physik, Föhringer Ring 6, D–80805 München, Germany
[5] Deutsches Elektronen-Synchrotron, DESY Zeuthen, Platanenallee 6, D–15738 Zeuthen, Germany

Abstract

Electroweak one-loop radiative corrections to the process $e^+e^- \to t\bar{t}$ are revisited. Two groups from Karlsruhe and Bielefeld/Zeuthen performed independent calculations of both (virtual and soft) QED contributions and weak virtual corrections. For the angular distribution an agreement of at least eight digits for the weak corrections and of at least six digits for additional photonic corrections is established.

* Work supported in part by the European Community's Human Potential Programme under contract HPRN-CT-2000-00149 Physics at Colliders.

† E-mails: fl@physik.uni-bielefeld.de, hahn@feynarts.de, hollik@particle.uni-karlsruhe.de, Tord.Riemann@desy.de, cs@particle.uni-karlsruhe.de, Anja.Werthenbach@desy.de

1 Introduction

At TESLA, one of the most important production processes will be top-pair production well above the production threshold (in the continuum)

$$e^+ \ (p_1) \ + \ e^- \ (p_2) \to t \ (p_3) \ + \ \bar{t} \ (p_4). \tag{1}$$

We expect several hundred thousand events, and the anticipated accuracy of the theoretical predictions to be a few per mille. What one has to calculate with such net precision is, of course, not only the two-fermion production process, but also the decay of the top quarks and the variety of quite different radiative corrections like real photonic bremsstrahlung, electroweak radiative corrections (EWRC), QCD corrections to the final state, and beamstrahlung. Potentially, new physics effects also have to be taken into account.

The state of the art at the time of the public presentation of the TESLA project has been reviewed in Part III of the Technical Design Report [1]. Since then, the community has made progress in several directions. In this note we report on recent developments in the description of the electroweak radiative corrections to (1). Several studies on this topic are available in the literature, e.g. [2, 3, 4, 5], but no special effort was undertaken to perform a detailed numerical comparison between the results of different collaborations. Quite recently, a recalculation of the electroweak corrections has been performed by a Bielefeld/Zeuthen group [6], and this calculation was compared in detail with the Karlsruhe results.[1]

We summarize this comparison together with a few remarks on the underlying projects.

2 One-loop EWRC to the reaction $e^+e^- \to t\bar{t}$

In this section we introduce the one-loop differential cross-section of the process $e^+e^- \to t\bar{t}$ in the Standard Model.

To start with, we first present the differential Born cross-section,

$$\frac{\mathrm{d}\sigma^{\mathrm{Born}}}{\mathrm{d}\cos\theta} \ = \ \left(1+\cos^2\theta\right)\sigma_T^0(s) + 2\cos\theta \ \sigma_{FB}^0(s) + \frac{4\,m_t^2}{s}\ \left(1-\cos^2\theta\right)\ \sigma_T^{0,m}(s), \tag{2}$$

with

$$\sigma_T^0(s) = \frac{\pi\alpha^2}{2s} c_t\beta_t \left[Q_e^2 Q_t^2 + 2Q_eQ_tv_ev_t \ \mathrm{Re}\,\chi_Z(s) + \left(v_e^2+a_e^2\right)\left(v_t^2+a_t^2\beta_t^2\right)|\chi_Z(s)|^2\right], \tag{3}$$

$$\sigma_{FB}^0(s) = \frac{\pi\alpha^2}{2s} c_t\beta_t^2 \left[2Q_eQ_ta_ea_t \,\mathrm{Re}\,\chi_Z(s) + 4v_ea_ev_ta_t\,|\chi_Z(s)|^2\right], \tag{4}$$

$$\sigma_T^{0,m}(s) = \frac{\pi\alpha^2}{2s} c_t\beta_t \left[Q_e^2 Q_t^2 + 2Q_eQ_tv_ev_t \ \mathrm{Re}\,\chi_Z(s) + \left(v_e^2+a_e^2\right)v_t^2\,|\chi_Z(s)|^2\right]. \tag{5}$$

[1] A series of numerical comparisons of the Bielefeld/Zeuthen group with the authors of [5] started in September 2001 and was later joined by the Karlsruhe group.

The Z propagator is contained in the factor

$$\chi_Z(s) = \frac{g^2}{4\,e^2\cos^2\theta_{\rm w}}\ \frac{s}{s-m_Z^2}, \tag{6}$$

$$m_Z^2 = M_Z^2 - iM_Z\Gamma_Z, \tag{7}$$

and we use the following conventions

$$Q_e = -1, \tag{8}$$

$$a_f = I_3^L(f) = \pm\frac{1}{2}, \tag{9}$$

$$v_f = a_f(1-4|Q_f|\sin^2\theta_{\rm w}), \tag{10}$$

together with

$$\beta_t = \sqrt{1-\frac{4\,m_t^2}{s}}, \tag{11}$$

and the colour factor $c_t = 3$ of the top quark. Including the virtual electroweak corrections and the soft photonic contributions it proves to be convenient to use the notation of complex-valued form factors, each of them related to some helicity-based matrix element. For the production of massive fermion pairs, the cross-section depends on six independent form factors,

$$\frac{{\rm d}\sigma}{{\rm d}\cos\,\theta} = \frac{\beta_t}{16\pi\,s}\,|\mathcal{M}_{\gamma+Z}|^2, \tag{12}$$

with

$$\begin{aligned}
|\mathcal{M}_{\gamma+Z}|^2 = &\left(U^2+T^2\right)\left(|{\rm F}_1^{11}|^2+|{\rm F}_1^{15}|^2+|{\rm F}_1^{51}|^2+|{\rm F}_1^{55}|^2\right) \\
&+\ 2\left(U^2-T^2\right){\rm Re}\left({\rm F}_1^{11}{\rm F}_1^{55*}+{\rm F}_1^{15}{\rm F}_1^{51*}\right) \\
&+\ 2\,m_t^2\,s\left(|{\rm F}_1^{11}|^2-|{\rm F}_1^{15}|^2+|{\rm F}_1^{51}|^2-|{\rm F}_1^{55}|^2\right) \\
&+\ 2\,\frac{m_t^2}{s}(U\,T-m_t^4)\,{\rm Re}\left({\rm F}_3^{11}{\rm F}_1^{11*}+{\rm F}_3^{51}{\rm F}_1^{51*}\right)\ +\mathcal{O}(\alpha^2)\,,
\end{aligned} \tag{13}$$

with $s=(p_1+p_2)^2$ and

$$T = \frac{s}{2}\,(1-\beta_t\,\cos\,\theta), \tag{14}$$

$$U = \frac{s}{2}\,(1+\beta_t\,\cos\,\theta). \tag{15}$$

The form factors appear in the decomposition of the matrix element according to

$$\mathcal{M}_{\gamma+Z} = \sum_{a,b=1,5}{\rm F_1}^{ab}\ \mathcal{M}_{1,ab}+{\rm F}_3^{11}\ \mathcal{M}_{3,11}+{\rm F}_3^{51}\ \mathcal{M}_{3,51}. \tag{16}$$

The matrix elements $\mathcal{M}_{3,11}$ and $\mathcal{M}_{3,51}$ emerge only in the calculation of the virtual corrections. Their interference with the Born amplitudes vanishes in the case of massless fermion pair production. The other matrix elements $\mathcal{M}_{1,ab}$ receive additional contributions from soft photon corrections. In Born approximation, the non-vanishing form factors are

$$\mathrm{F}^{11}_{1,\mathrm{B}} = \left(e^2\,\chi_Z(s)\,v_e\,v_t + e^2\,Q_e\,Q_t\right)\,/\,s, \tag{17}$$
$$\mathrm{F}^{15}_{1,\mathrm{B}} = -e^2\,\chi_Z(s)\,v_e\,a_t\,/\,s, \tag{18}$$
$$\mathrm{F}^{51}_{1,\mathrm{B}} = -e^2\,\chi_Z(s)\,v_t\,a_e\,/\,s, \tag{19}$$
$$\mathrm{F}^{55}_{1,\mathrm{B}} = e^2\,\chi_Z(s)\,a_e\,a_t\,/\,s. \tag{20}$$

For completeness, we give also the matrix elements

$$i\,\mathcal{M}_{1\,ab} = [\bar{v}(p_1)\;\gamma^\mu\,g_a\,u(p_2)\;]\;[\bar{u}(p_3)\;\gamma_\mu\,g_b\,v(p_4)\;], \qquad a,b = 1,5, \tag{21}$$

where $g_1 = 1$ and $g_5 = \gamma_5$. For massive loop corrections, two additional structures have to be added

$$i\,\mathcal{M}_{3,11} = [\bar{v}(p_1)\;\mathbb{1}\,u(p_2)\;]\;[\bar{u}(p_3)\;\not{p}_2\,\mathbb{1}\,v(p_4)\;], \tag{22}$$
$$i\,\mathcal{M}_{3,51} = [\bar{v}(p_1)\;\not{p}_3\,\gamma_5\,u(p_2)\;]\;[\bar{u}(p_3)\;\mathbb{1}\,v(p_4)\;]. \tag{23}$$

In Appendix A we give the collection of all Feynman diagrams relevant at one-loop level for the calculation in the 't Hooft–Feynman gauge. Ultra-violet (UV) divergences were treated within dimensional regularization. For renormalization the on-shell scheme was used [7]. Infra-red (IR) divergences cancel analytically between the soft photon emission and the diagrams with virtual photons. This leads to a residual dependence of the cross-section on the maximal soft-photon energy, which has been arbitrarily chosen to be $E_\gamma^{\max} = \sqrt{s}/10$. Of course, after including real hard photonic bremsstrahlung this dependence disappears.

In the on-shell renormalization scheme the weak mixing angle is defined by the weak boson masses. In this calculation the coupling constant g (6) is expressed by the electric charge and the weak mixing angle.

$$\sin^2\theta_W = 1 - \frac{M_W^2}{M_Z^2}, \tag{24}$$
$$g = \frac{e}{\sin\theta_\mathrm{w}}. \tag{25}$$

2.1 The Karlsruhe Approach

The Karlsruhe calculations have a long history dating back to the late 1980s, following the formulation worked out in [8, 9]. We shall not describe them here in detail. They use the software packages `FeynArts` [10, 11], `FormCalc` [12], and `LoopTools` [12], the latter of which is based on the `FF` library [13]. The calculations follow the scheme described in [14]: the diagrams are first generated with FeynArts, the resulting amplitudes are analytically simplified with FormCalc, whose output is then converted to a Fortran program which is linked with the LoopTools library to produce e.g. cross-sections. This process takes only a few minutes and is highly automated.

Results of calculations performed in this way have been made available on *The HEP Process Repository* Web page [15]. The actual codes used for comparison in this paper have been taken from there. In particular we used the files `eett_sm.tar.gz` and `eett_smnoqed.tar.gz`.

We just mention that a file with the virtual one-loop corrections in the MSSM, `eett_mssm.tar.gz`, is also obtainable.

2.2 The Bielefeld/Zeuthen Approach

The Bielefeld/Zeuthen group utilized the program package `DIANA` [16, 17], which is a `FORM` interface for the package `qgraph` [18] for the creation of all the contributing Feynman diagrams to a given process.

The output of `DIANA` is a sample of symbolic expressions which then were prepared for the integration of the loop momenta with `FORM` [19]. Two independent calculations which differ in many respects have been performed. In one of them, dimensional regularization is used for UV and IR divergences, while in the other the IR divergences are regularized by a finite, small photon mass. The resulting expressions in terms of Passarino-Veltman functions are calculated with a Fortran code, using two libraries of one-loop functions: the dimensionally-regularized version uses `LoopTools` [12] with minor additions, the other one the package `FF` [13]. On-shell renormalization is performed following [20]. To eliminate the IR divergence of the virtual photonic contributions soft photon bremsstrahlung has been added; we followed the techniques described in [21].

The Fortran program `topfit` provides two possible outputs: Firstly the differential cross-section (and derived observables like total cross-section or forward-backward asymmetry), secondly six independent form factors in a given helicity basis, as introduced above, designed to be used in a Monte-Carlo program.

It is worth mentioning that `topfit` is equipped to calculate the hard real photon corrections to the differential cross-section.

3 Numerical Results

The comparison of the two calculations is chosen to be performed on the level of the differential cross-section. We focus in particular on the following four contributions

- $\left[\frac{\mathrm{d}\sigma}{\mathrm{d}\cos\theta}\right]_{\mathrm{Born}}$: Born cross-section which serves as a cross check of input parameters and conventions.
- $\left[\frac{\mathrm{d}\sigma}{\mathrm{d}\cos\theta}\right]_{\mathrm{QED}}$: These numbers contain the Born cross-section plus the interference of Born (s-channel γ and Z exchange) with one-loop virtual QED diagrams plus the absolute square of real soft photon radiation. No vacuum polarization diagrams, nor counter–diagrams, of the photon are taken into account, i.e. the running of the electromagnetic coupling constant is not included. It is assumed that this can be easily accounted for, including the variety of higher order corrections, by using the corresponding value of α.
- $\left[\frac{\mathrm{d}\sigma}{\mathrm{d}\cos\theta}\right]_{\mathrm{weak}}$: The interference of Born (s-channel γ and Z exchange) with one-loop virtual pure weak diagrams is shown. As before, the Born cross-section is added to the one-loop correction. The running of the electromagnetic coupling constant is included here. Renormalization is performed in the on-shell scheme and self-energy diagrams are taken into account as well.
- $\left[\frac{\mathrm{d}\sigma}{\mathrm{d}\cos\theta}\right]_{\mathrm{SM}}$: All previous parts of the calculation are put together, i.e. the complete electroweak one-loop plus Born differential cross-section is given within the Standard Model.

All numbers in the following tables were obtained making use of the input parameters

$$
\begin{aligned}
&\Gamma_Z = 0\ , && \alpha = \tfrac{e^2}{4\pi} = 1/137.03599976\ , && E_\gamma^{\max} = \sqrt{s}/10\ , \\
&M_W = 80.4514958\,\mathrm{GeV}\ , && M_Z = 91.1867\,\mathrm{GeV}\ , && M_H = 120\,\mathrm{GeV}\ , \\
&m_e = 0.00051099907\,\mathrm{GeV}\ , && m_t = 173.8\,\mathrm{GeV}\ , && m_b = 4.7\,\mathrm{GeV}\ , \\
&m_\mu = 0.105658389\,\mathrm{GeV}\ , && m_u = 0.062\,\mathrm{GeV}\ , && m_d = 0.083\,\mathrm{GeV}\ , \\
&m_\tau = 1.77705\,\mathrm{GeV}\ , && m_c = 1.5\,\mathrm{GeV}\ , && m_s = 0.215\,\mathrm{GeV}\ .
\end{aligned}
\qquad (26)
$$

Effective quark masses reproducing the hadronic vacuum polarization contribution $\Delta\alpha_h$ with a sufficiently high accurancy have been chosen [22, 7]. As mentioned, the photon energy cut $E_\gamma^{\max}$ is an arbitary quantity entering the final result if the radiation of hard photons in not taken into account.

The numerical values of the differential cross-sections have been calculated at three typical Next–Linear–Collider energies.

$\sqrt{s} = 500$ GeV:

$\cos\theta$	$\left[\frac{d\sigma}{d\cos\theta}\right]_{\mathrm{Born}}$	$\left[\frac{d\sigma}{d\cos\theta}\right]_{\mathrm{QED}}$	$\left[\frac{d\sigma}{d\cos\theta}\right]_{\mathrm{weak}}$	$\left[\frac{d\sigma}{d\cos\theta}\right]_{\mathrm{SM}}$
-0.9	0.1088 3919 4075	0.09866 4244	0.1242 59037 1	0.1140 8409
	0.1088 3919 4075	0.09866 4251	0.1242 59037 6	0.1140 8409
-0.5	0.1422 7506 9392	0.1285 0789	0.1568 48371 9	0.1430 8119
	0.1422 7506 9392	0.1285 0791	0.1568 48371 8	0.1430 8121
0.	0.2254 7046 4032	0.2023 9165	0.2402 6680 4	0.2171 8799
	0.2254 7046 4033	0.2023 9167	0.2402 6680 3	0.2171 8801
0.5	0.3546 6647 0331	0.3151 1721	0.3688 8650 7	0.3293 3725
	0.3546 6647 0332	0.3151 1723	0.3688 8650 5	0.3293 3727
0.9	0.4911 4371 5766	0.4307 1433	0.5033 3751 2	0.4429 0813
	0.4911 4371 5767	0.4307 1438	0.5033 3750 8	0.4429 0817

$\sqrt{s} = 700$ GeV:

$\cos\theta$	$\left[\frac{d\sigma}{d\cos\theta}\right]_{\mathrm{Born}}$	$\left[\frac{d\sigma}{d\cos\theta}\right]_{\mathrm{QED}}$	$\left[\frac{d\sigma}{d\cos\theta}\right]_{\mathrm{weak}}$	$\left[\frac{d\sigma}{d\cos\theta}\right]_{\mathrm{SM}}$
-0.9	0.05033 2867 3357	0.04534 6964	0.05697 6919 7	0.05199 1017
	0.05033 2867 3357	0.04534 6950	0.05697 6920 1	0.05199 1003
-0.5	0.06658 1166 2000	0.05993 8998	0.07224 8491 7	0.06560 6323
	0.06658 1166 2001	0.05993 8983	0.07224 8491 7	0.06560 6308
0.	0.1237 4052 8515	0.1106 4935	0.1280 5635 7	0.1149 6518
	0.1237 4052 8515	0.1106 4932	0.1280 5635 6	0.1149 6514
0.5	0.2218 4321 1646	0.1955 2870	0.2224 6611 4	0.1961 5161
	0.2218 4321 1646	0.1955 2863	0.2224 6611 3	0.1961 5153
0.9	0.3298 0454 9138	0.2844 3993	0.3245 1514 8	0.2791 5053
	0.3298 0454 9138	0.2844 3984	0.3245 1514 5	0.2791 5044

$\sqrt{s} = 1000$ GeV:

$\cos\theta$	$\left[\frac{d\sigma}{d\cos\theta}\right]_{\rm Born}$	$\left[\frac{d\sigma}{d\cos\theta}\right]_{\rm QED}$	$\left[\frac{d\sigma}{d\cos\theta}\right]_{\rm weak}$	$\left[\frac{d\sigma}{d\cos\theta}\right]_{\rm SM}$
-0.9	0.02278 5423 2732	0.02036 5835	0.02552 1285	0.02310 1698
	0.02278 5423 2732	0.02036 5843	0.02552 1286	0.02310 1705
-0.5	0.02978 2131 1031	0.02674 1651	0.03186 3489	0.02882 3009
	0.02978 2131 1031	0.02674 1664	0.03186 3489	0.02882 3022
0.	0.06118 0067 4224	0.05453 9323	0.06159 1613	0.05495 0869
	0.06118 0067 4224	0.05453 9344	0.06159 1613	0.05495 0889
0.5	0.1177 4694 9888	0.1031 1623	0.1140 47686	0.09941 6970
	0.1177 4694 9888	0.1031 1626	0.1140 47685	0.09941 6996
0.9	0.1811 2209 7086	0.1540 3818	0.1713 46193	0.1442 6227
	0.1811 2209 7086	0.1540 3824	0.1713 46191	0.1442 6233

Table 1: The content of the tables is explained in the text, the upper and lower numbers correspond to the Karlsruhe and Bielefeld/Zeuthen approach, respectively.

From Table 1 it is evident that the numerics of the weak virtual corrections are perfectly controlled with a gross agreement of the two approaches by at least eight digits.

The pure photonic corrections agree to at least six digits. The disagreement beyond the sixth decimal has been traced back to the treatment of the soft real photons in the `eett_sm.tar.gz` package. [2] The net result of the comparison being highly satisfactory, we did not push for more digits agreement.

Finally, it has to be pointed out that we control here only what is often called the *technical precision* of a calculation, not to be confused with the precision of the prediction of some observable to be confronted with some realistic measurement.

4 Summary

We have demonstrated an agreement of six to eight digits between the calculations of the Karlsruhe group and the Bielefeld/Zeuthen group for electroweak virtual and soft photonic corrections to the reaction $e^+e^- \to t\bar{t}$ at the one-loop level.

Naturally the claim of completeness of this calculation can only be applied to the *electroweak* corrections and only at one-loop accuracy. In particular the inclusion of QCD corrections [1] and the finite life time of the top quarks have to be taken into account. To what extent higher-order weak corrections will be needed depends crucially on the expected experimental accuracy. Certainly, it is desirable to partially extend the calculations to higher-order effects, where a special emphasis could be given to large mass effects [7] and to the so-called Sudakov logarithms [24], which constitute the leading contributions at

[2] The `topfit` part was analytically and numerically cross-checked against [23].

the next order in perturbation theory. Finally, needless to mention that various higher-order photonic corrections have to be added in high-precision numerical approach.

5 Acknowledgments

We would like to thank D. Bardin, P. Christova, and L. Kalinovskaya for informal discussions.

Appendix

A Feynman diagrams

In cases where several particles are listed for a propagator, there is one diagram for each combination of particles. On fermion lines, an f_i stands for $\{e, \mu, \tau, u, c, t, d, s, b\}$ and a ν_i for $\{\nu_e, \nu_\mu, \nu_\tau\}$.

Born diagrams:

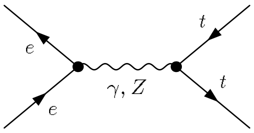

Counter-term diagrams:

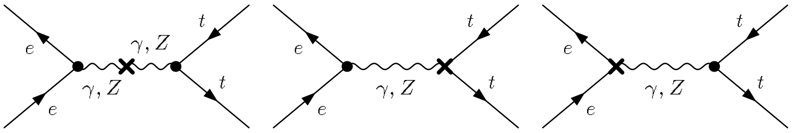

Self-energy diagrams:

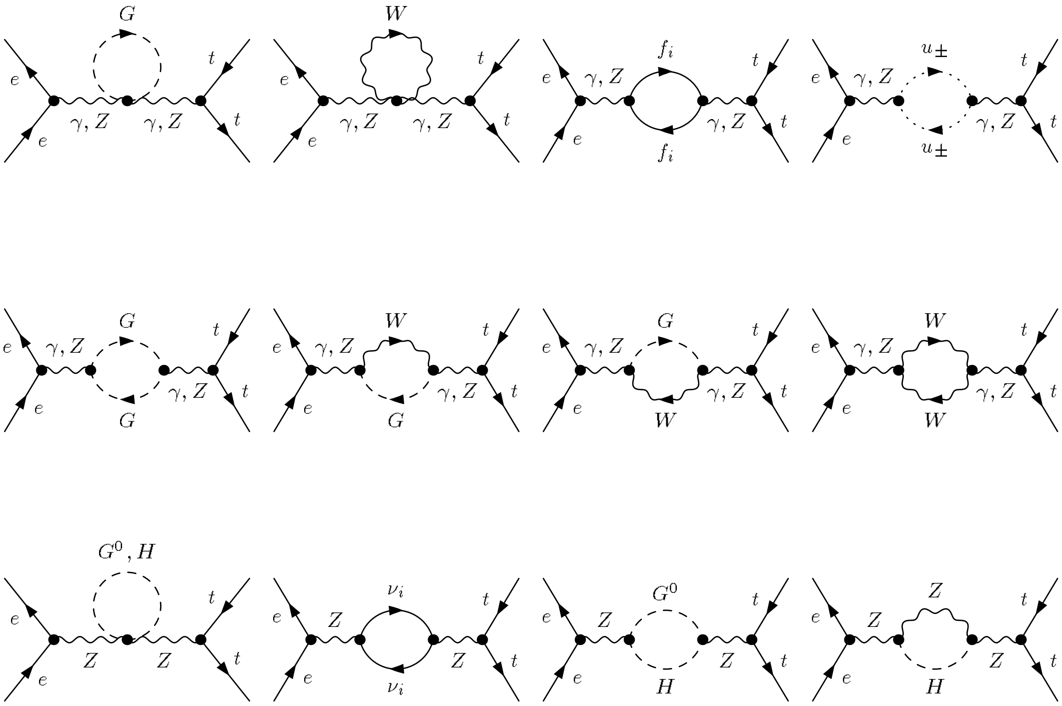

Vertex diagrams:

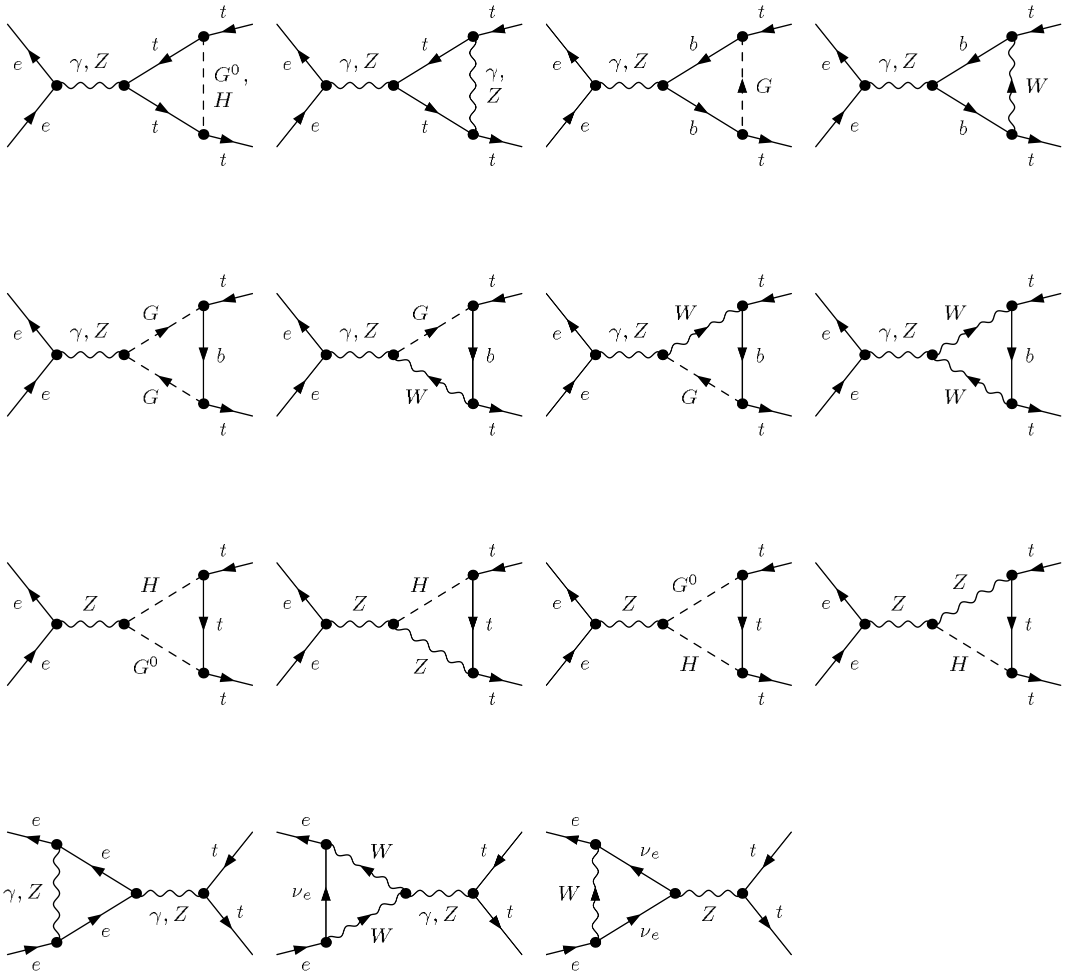

Real-photon-emission diagrams:

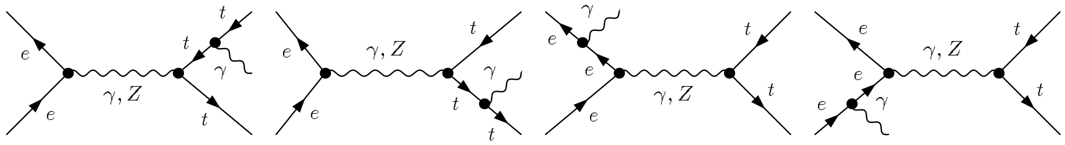

Box diagrams:

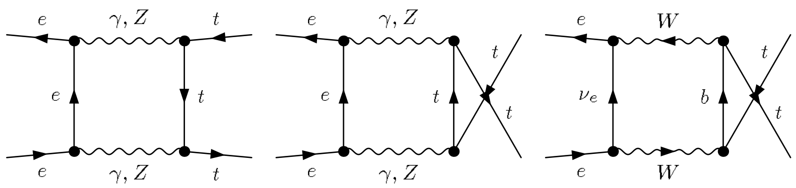

References

[1] ECFA/DESY LC Physics Working Group (J. Aguilar-Saavedra et al.), "TESLA Technical Design Report Part III: Physics at an e^+e^- Linear Collider", preprint DESY 2001–011 (2001), `hep-ph/0106315`.

[2] J. Fujimoto and Y. Shimizu, *Mod. Phys. Lett.* **3A** (1988) 581.

[3] W. Beenakker, S. van der Marck and W. Hollik, *Nucl. Phys.* **B365** (1991) 24–78.

[4] W. Hollik and C. Schappacher, *Nucl. Phys.* **B545** (1999) 98–140.

[5] D. Bardin, L. Kalinovskaya and G. Nanava, "An electroweak library for the calculation of EWRC to $e^+e^- \to f\bar{f}$ within the CalcPHEP project", Dubna preprint JINR E2–2000–292 (2000), `hep-ph/0012080,` v.2 (12 Dec 2001).

[6] J. Fleischer, A. Leike, T. Riemann and A. Werthenbach, Fortran program `topfit.F` v.0.9 (16 Jan 2002), to be published.

[7] D. Bardin *et al.*, "Electroweak working group report", in *Reports of the Working Group on Precision Calculations for the Z Resonance,* report CERN 95–03 (1995) (D. Bardin, W. Hollik and G. Passarino, eds.), pp. 7–162, `hep-ph/9709229`.

[8] M. Böhm, H. Spiesberger and W. Hollik, *Fortsch. Phys.* **34** (1986) 687–751.

[9] A. Denner, *Fortschr. Phys.* **41** (1993) 307–420.

[10] J. Küblbeck, M. Böhm and A. Denner, *Comput. Phys. Commun.* **60** (1990) 165–180.

[11] T. Hahn, *Comput. Phys. Commun.* **140** (2001) 418–431.

[12] T. Hahn and M. Perez-Victoria, *Comput. Phys. Commun.* **118** (1999) 153–165.

[13] G. van Oldenborgh, *Comput. Phys. Commun.* **66** (1991) 1–15.

[14] T. Hahn, *Nucl. Phys. Proc. Suppl.* **89** (2000) 231–236.

[15] T. Hahn and C. Schappacher, The HEP Process Repository, `http://www.hep-processes.de`.

[16] M. Tentyukov and J. Fleischer, *Comput. Phys. Commun.* **132** (2000) 124–141.

[17] J. Fleischer and M. Tentyukov, "A Feynman diagram analyser DIANA: Graphic facilities", in: P. Bhat and M. Kasemann (eds.), Proc. of the VIIth Int. Workshop ACAT 2000, Batavia, USA, 16-20 Oct. 2000, AIP Conference Proceedings (Melville, New York, 2001), vol. 583, p. 193, `hep-ph/0012189`.

[18] P. Nogueira, *J. Comput. Phys.* **105** (1993) 279–289.

[19] J. A. M. Vermaseren, Symbolic manipulation with FORM (Amsterdam, Computer Algebra Nederland, 1991).

[20] J. Fleischer and F. Jegerlehner, *Phys. Rev.* **D23** (1981) 2001–2026.

[21] A. Akhundov, D. Bardin, L. Kalinovskaya and T. Riemann, *Fortschritte Phys.* **44** (1996) 373–482.

[22] S. Eidelman and F. Jegerlehner, *Z. Phys.* **C67** (1995) 585–6.502.

[23] W. Beenakker, "Electroweak corrections: Techniques and applications", Ph.D. thesis, Univ. Leiden, 1989.

[24] W. Beenakker and A. Werthenbach, "Electroweak two-loop Sudakov logarithms for on-shell fermions and bosons", DESY preprint 01–131 (2001), `hep-ph/0112030`.